

# The microstructure and hardness of molybdenum powders consolidated by plasma pressure compaction<sup>☆</sup>

T.S. Srivatsan<sup>a,\*</sup>, B.G. Ravi<sup>a</sup>, A.S. Naruka<sup>a</sup>, L. Riester<sup>b</sup>, M. Petraroli<sup>c</sup>, T.S. Sudarshan<sup>d</sup>

<sup>a</sup> Department of Mechanical Engineering, Auburn Science and Engineering Center, The University of Akron, Akron, OH 44325-3903, USA

<sup>b</sup> Mechanical Characterization and Analysis Group, High-Temperature Materials Laboratory, Oak Ridge National Laboratory, Oak Ridge, TN 37831, USA

<sup>c</sup> The Timken Research, The Timken Company, 1835 Dueber Avenue S.W., P.O. Box 6930, Canton, OH 44706-6930, USA

<sup>d</sup> Materials Modification Inc., No. 2929-P1, Eskridge Road, Fairfax, VA 22031, USA

Received 1 February 2000; received in revised form 28 April 2000; accepted 28 April 2000

## Abstract

Bulk molybdenum samples were prepared by consolidating molybdenum powders using the technique of plasma pressure compaction (P<sup>2</sup>C). The specimens were obtained by consolidating the powder particles under conditions of pulse and no-pulse and at two different temperatures. Results reveal that pulsing of the powders prior to consolidation had little influence on microhardness when compared to the samples that were obtained by consolidating the powder particles under no-pulse. Both nanohardness and microhardness measurements revealed a marginal decrease with an increase in temperature of compaction. The influence of processing variables on microstructural development and hardness is presented and discussed. © 2001 Elsevier Science S.A. All rights reserved.

**Keywords:** Molybdenum; Processing; Microstructure; Density; Hardness

## 1. Introduction

Molybdenum has a body-centered cubic crystal structure with a melting point of 2610°C and a density of 10.22 g/cm<sup>3</sup> and is an important refractory metal. The refractory properties of molybdenum reflect the high strength of interatomic bonding resulting from an overlap of the 4d orbital and the number of available bonding electrons [1]. Only tungsten and tantalum among the available high-temperature metals exceed the melting point of molybdenum. This makes molybdenum a material having “hot strength”. Besides, it has acceptable ambient temperature ductility and a ductile-to-brittle transition temperature significantly lower than that of tungsten [2]. The density of molybde-

num is approximately 50% that of tungsten and 62% that of tantalum. Because of its low density (compared to tungsten and tantalum), the resultant specific strength (ratio of tensile strength to density) is high. Molybdenum also possesses a much greater specific heat (0.276 kJ/kg K) than either tungsten (0.131 kJ/kg K) or tantalum (0.139 kJ/kg K) [1]. The combination of thermal conductivity (135 W/m K) and specific heat (0.276 kJ/kg K) of molybdenum makes it a potentially attractive and viable choice for components that must resist thermal shock and fatigue. Also, the relatively low thermal neutron cross-section of molybdenum makes it suitable for nuclear applications. In fact, the unique combination of physical, chemical and mechanical properties of molybdenum makes it an ideal material for a spectrum of engineering applications where high temperature capability, weight considerations and ductility are key issues [1–4].

During the last two decades, molybdenum and its alloys have received increased interest for defense-related applications where its mechanical properties under high-strain rate deformation have proven desirable [5]. However, in more recent years, molybdenum has also found use in thermal management of silicon devices. The thermal expansion of molybdenum is close to that of silicon, particu-

<sup>☆</sup> Research jointly supported by the National Science Foundation (grant no. NSF-CMS: 980-2185), the State of Ohio Board of Regents (Columbus, OH) and the U.S. Department of Energy, Assistant Secretary for Energy Efficiency and Renewable Energy, Office of Transportation Technologies, as part of the High-Temperature Materials Laboratory User Program, with Lockheed Martin Energy Research, under contract DE-AC05-84OR21400.

\* Corresponding author. Tel.: +1-330-972-6196; fax: +1-330-972-6027.

E-mail address: tsrivatsan@uakron.edu (T.S. Srivatsan).

larly over the temperature range typically encountered in solid-state device applications [1,5]. It also finds wide use in vacuum furnaces, primarily because of its low vapor pressure in the operating temperature and pressure range of the furnaces.

Sintering temperatures for the refractory metals are usually very high. For example, typical sintering temperature for tungsten ranges up to 3000°C for a time period of 15–30 min [6,7]. Prolonged time periods are often needed when sintering at low temperatures, i.e., to achieve around 90% of the theoretical density of tungsten, it would take 20 h at a temperature of 1027°C. To achieve nearly full density in short processing time intervals, while concurrently minimizing grain growth-related degradation in mechanical properties, a few non-conventional techniques have been reported for the consolidation of high-temperature materials. Explosive consolidation [8–11], ceracon rapid omni-directional (ROC) [12–14], plasma-activated sintering (PAS) [15,16] and microwave sintering [17,18] are a few of the rapid consolidation techniques reported in the open literature. In microwave sintering, the material absorbs microwaves and is rapidly heated to very high temperature in a short time period with resultant rapid consolidation. Consolidation by shock waves is achieved by the preferential short-duration deposition of energy on particle surfaces through mechanisms of plastic deformation and friction between particles [10,11]. Shock wave consolidation can be achieved either by detonating explosives or producing shock waves by the high-velocity impact of projectiles. Jones et al. [15] and Groza et al. [16] reported using PAS of tungsten and aluminum nitride

(AlN) powders in a short time period with a minimum of changes in intrinsic microstructural features.

An economically affordable, efficient and viable approach is plasma pressure consolidation. This is a rapid densification process developed by Materials Modification (MMI, Fairfax, VA, USA) that has the potential to minimize grain growth by enhancing particle sinterability through the conjoint action of particle surface activation and rapid heating for very short times (minutes vs. hours) when compared with other conventional processes [19,20]. The technique of plasma pressure compaction (henceforth referred to as P<sup>2</sup>C) is a short-time, high-temperature, low-pressure process that has been successfully used to compact coarse (> 20 μm), fine (between 1 and 20 μm) and ultrafine (nanometer) metallic, intermetallic and ceramic powders to full density and near-net shapes [19]. The purpose of this research article is to examine the influence of processing conditions on the microstructure, density and microhardness of bulk molybdenum specimens made by consolidating powder particles.

## 2. Experimental techniques

### 2.1. Sample preparation

Molybdenum powders, with an average particle size of 47 μm, were consolidated by the technique of P<sup>2</sup>C. In this technique, molybdenum powders were poured into a graphite die without any additive or binder. A constant uniaxial pressure was applied to the powders through the

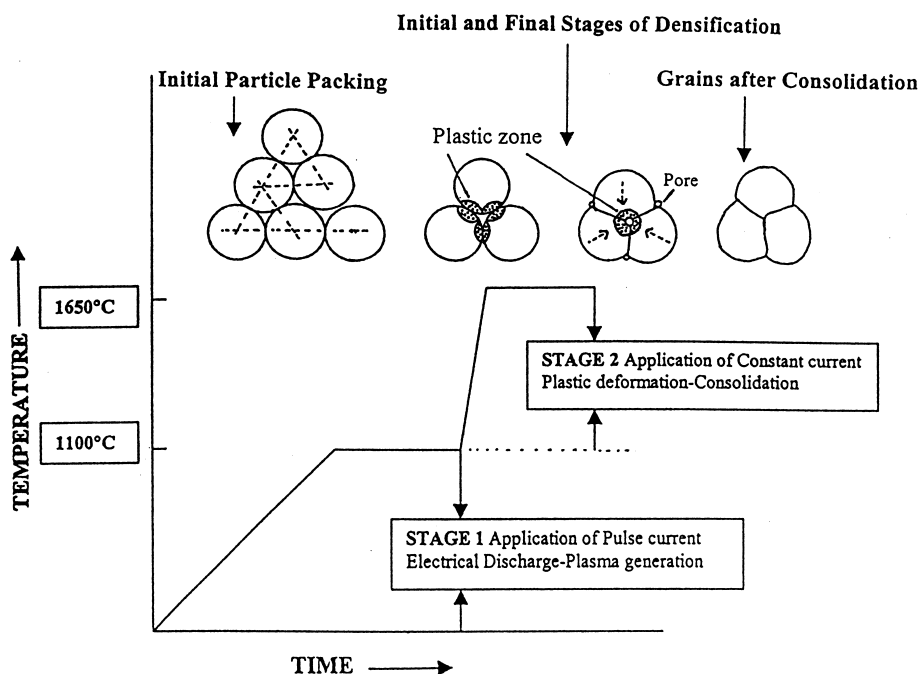


Fig. 1. Schematic of time–temperature cycle followed in the compaction process and different stages of consolidation.

Table 1  
Summary of the process conditions used and density of the bulk samples

Sample	Particle size ( $\mu\text{m}$ )	Process conditions				Density (%)
		Pulse	Temperature ( $^{\circ}\text{C}$ )	Time (min)	Pressure (MPa)	
1	47	Yes	1650	1.0	48	98.50
2	47	No	1650	1.0	48	98.00
3	47	Yes	1600	1.5	40	96.00
4	47	No	1650	1.5	40	93.00
5	47	Yes	1650	2.0	40	98.30

graphite plungers. A schematic of the time–temperature cycle and the two stages involved in consolidation, assuming the powder particles to be spherical, is shown in Fig. 1. When pulsed electrical power is applied, the current does not flow freely through the powder compact since an effective current path has not, as yet, been established. The oxide layer on the surface of the molybdenum powder particle acts as an insulator at the particle contact. This causes a charge buildup at the interparticle gaps (between the powder particles), which causes one particle to be charged negatively with respect to the other particles that are in contact with it. As the charge builds up, the voltage difference becomes sufficiently large to generate sparks that trigger an ionization process. The resultant interparticle plasma serves to activate the surface of the powder particles by removing the oxide and other contaminants. At this stage, the powder compact was heated to  $\approx 1100^{\circ}\text{C}$  and any adsorbed gas and/or moisture was released. This was indicated by drop in the initial vacuum level ( $10^{-3}$  Torr). At this stage, an external uniaxial pressure of approximately 20 MPa was applied so as to facilitate sufficient current path through the powder compact. Application of the pulse current ends once the vacuum has reached its initial value. In the following stage, a constant current of approximately 4000 A was applied so as to achieve a temperature of  $1650^{\circ}\text{C}$ . Direct application of the current and an external uniaxial pressure (now 48 MPa) serves to

accelerate densification of the material by inducing resistance heating and causing plastic deformation at the interparticle contact surfaces. The resistance heat serves to concentrate the heat at interparticle points of contact and the concurrent application of light pressure results in densification of the compact. The consolidation temperature was fixed at  $1650^{\circ}\text{C}$ . Since graphite dies (of diameter 26 mm) were used for consolidation, the maximum pressure used was limited to 48 MPa. To establish the influence of pressure on compaction, certain experiments were also performed at a lower pressure (40 MPa). The consolidated samples measured 25 mm in diameter and 15 mm in thickness. The consolidation conditions and relative density of the samples are summarized in Table 1. In an attempt to establish the influence of a DC pulse on consolidation, samples were made under conditions of pulse and no-pulse. A schematic of the plasma pressure consolidation equipment is shown in Fig. 2.

## 2.2. Microstructural characterization

The as-consolidated samples were prepared for examination in the optical and scanning electron microscope (SEMs) to identify: (a) grain size and morphology, and (b) the presence and distribution of processing-related defects. The defect features include: (1) irregular surface cracks, (2) string-like and angular features, and (3) microscopic pores and voids. Sample preparation involved an initial wet grind and coarse polish on progressively finer grades of Buehler's Ultra Plan™, Ultra Pad™ and Texmat™ pol-

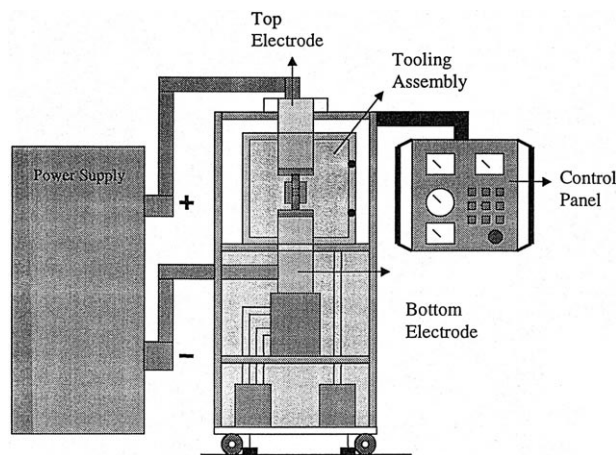


Fig. 2. A schematic of the P<sup>2</sup>C set up.

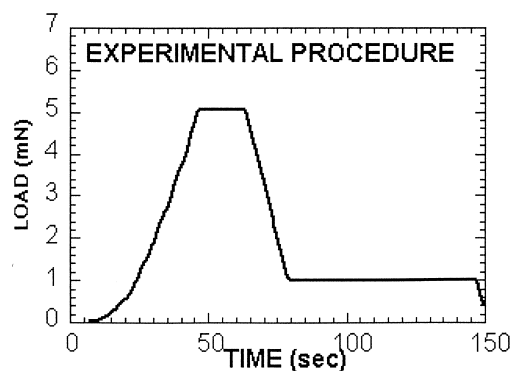


Fig. 3. A typical load time sequence (peak load = 120 mN).

ishing cloths using diamond suspension as the lubricant. Finish polishing was achieved using 1- $\mu\text{m}$  diamond paste and water as the lubricant. The as-polished samples were chemically etched using Murakami's reagent (a solution mixture of 10 g potassium ferricyanide, 10 g of sodium hydroxide, and 100 ml of distilled water). The etched samples were observed in an optical microscope and photographed using standard brightfield illumination. The polished and etched samples were also examined in a SEM with the objective of determining the morphology and distribution of artifacts, i.e., residual porosity. Precise density measurements of the consolidated bulk molybdenum samples were made using the Archimedes' principle according to ASTM Standard B328-94.

### 2.3. Indentation procedures

Ultra-low load indentations were performed on the samples using the nanoindentation technique [21,22]. The Nano

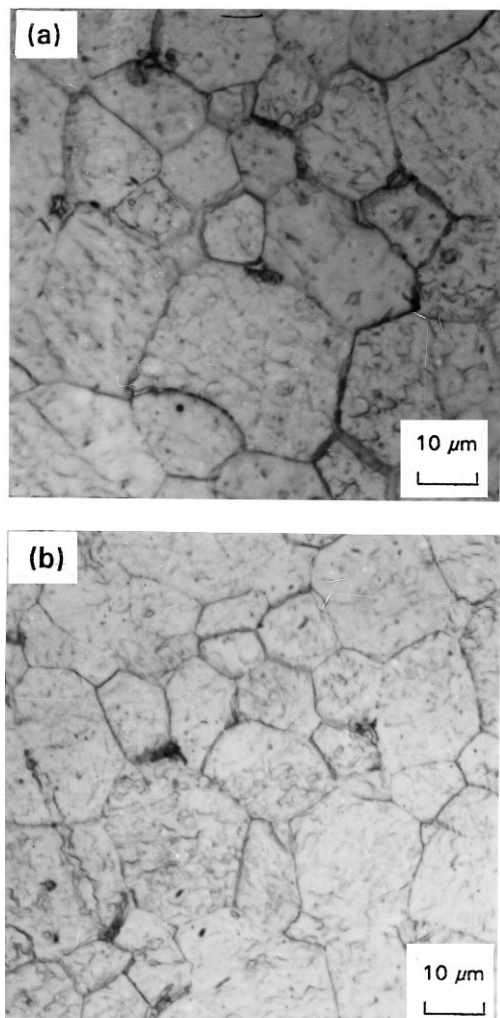


Fig. 4. Optical micrographs showing the overall grain structure of samples consolidated at pressure of 48 MPa at 1650°C: (a) sample 1 (pulse); (b) sample 2 (no-pulse).

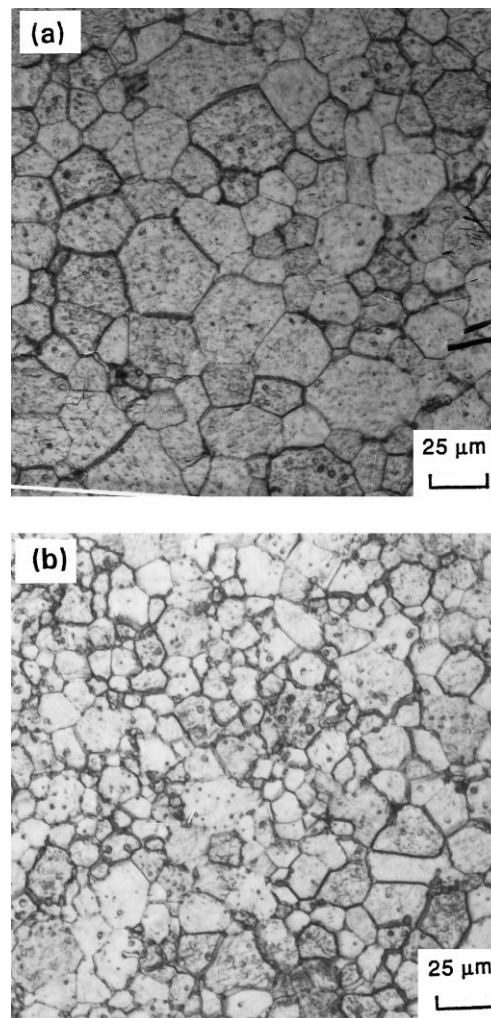


Fig. 5. Optical micrographs showing the overall grain structure of the samples consolidated at pressure of 40 MPa at 1600°C: (a) sample 3 (pulse); (b) sample 4 (no-pulse).

Indenter II (Nano Indenter is a registered trademark of Nano Instruments, at Oak Ridge, TN, USA) at the High-Temperature Materials Laboratory, Oak Ridge National Laboratory, has a displacement resolution of 0.16 nm and a load resolution of 0.3  $\mu\text{N}$ . Indentations were made using a three-sided diamond pyramid Berkovich indenter [23]. The indenter has nearly the same area-to-depth ratio as the four-sided Vickers, which allows these hardness values to be directly compared [22]. The nanoindenter is equipped with a numerically controlled loading unit and a high-resolution measurement system for measuring the indentation depth. Indentation positions were individually located on the sample surface using an optical microscope with a 1500 $\times$  magnification. The sample table encoded the positions with reasonable accuracy, enabling the indentations to be positioned well within the grain interior and away from grain boundaries, scratches and porosity. The depth and rates of loading and unloading (Fig. 3) were programmed, and a pattern for a set of ten indents was

established. On account of the nature of the material being evaluated (hard metal: molybdenum), each indentation sequence was composed of an approach segment (segment 1) to locate the surface. The sample was loaded to a constant depth during segment 2 and held at that stage. The loading period is referred to as segment 3. Segment 4 was the unloading segment. Since in this test sequence a fixed penetration depth was selected, the load varied as a direct function of hardness rather than penetration depth as is the

case of standard microhardness techniques. This procedure has the advantage of producing indents of constant size and depth. The indentation system also has the ability to continuously measure contact stiffness during indentation from which both hardness and Young's Modulus computations were carried out using the method described by Oliver and Pharr [22].

Using a Buehler Micromet II microhardness tester, Vickers microhardness ( $H_v$ ) measurements, on polished

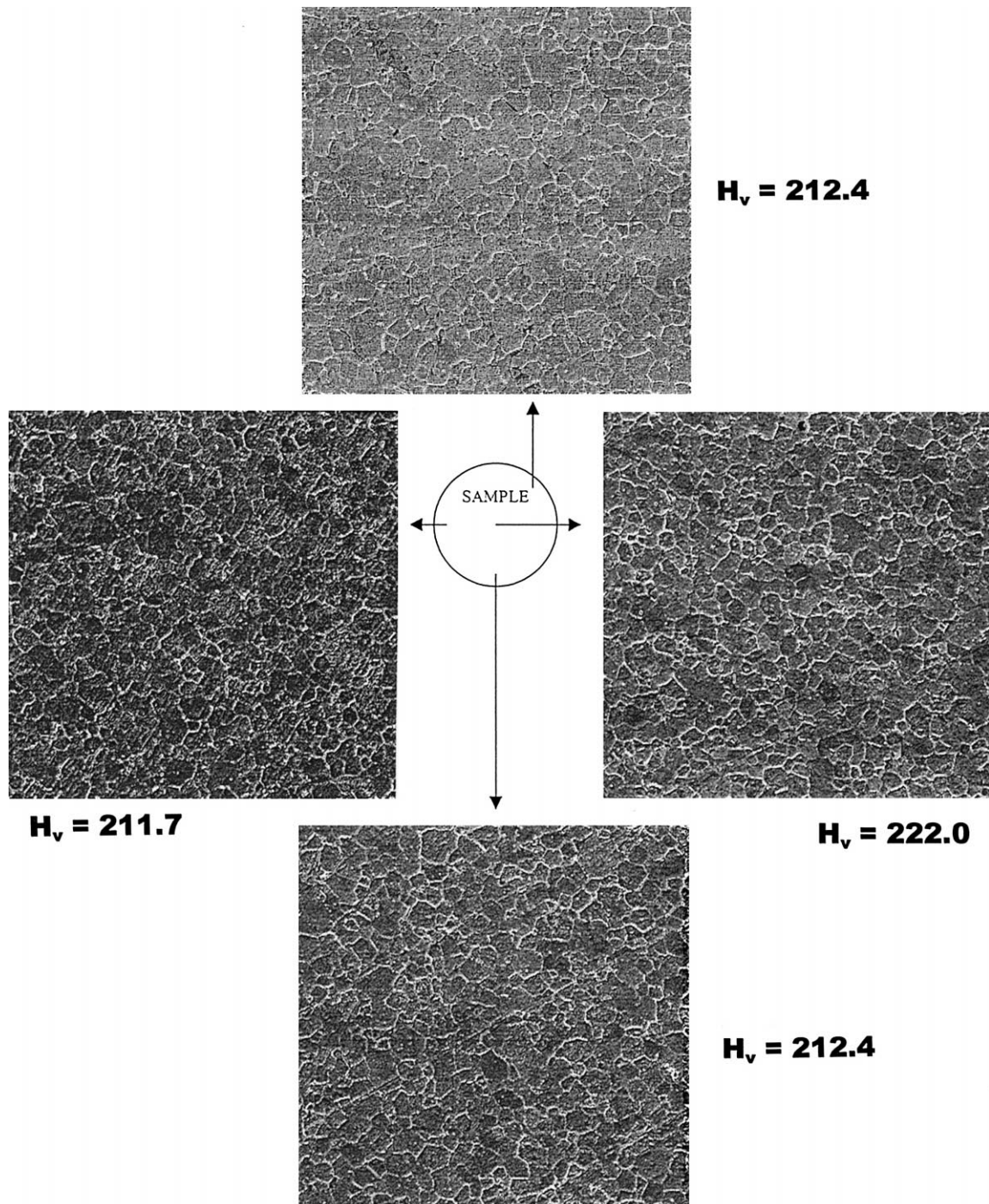


Fig. 6. Scanning electron micrographs showing microstructure at different locations on the polished-etched surface of sample 3.

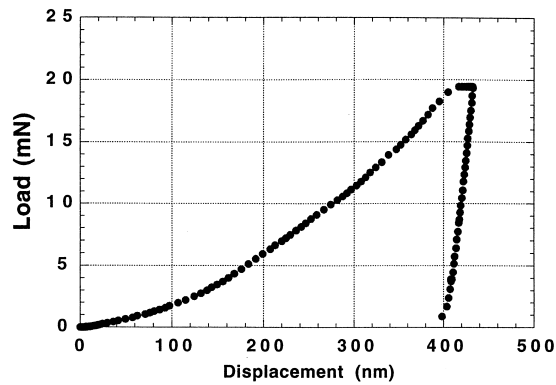


Fig. 7. Typical load vs. indenter displacement for the highest peak load experiment performed on mechanically polished molybdenum sample.

surfaces of the as-compacted sample(s), were made using a load of 100 g and a dwell time of 15 s at room temperature. Each hardness value represents the average of five such measurements and is reported as pressure in gigaPascal.

### 3. Results and discussion

#### 3.1. Microstructure

The microstructure of the consolidated samples in both as-polished and polished plus etched conditions was imaged using (a) brightfield illumination in an optical microscope at low magnifications, and (b) a SEM at higher magnifications. Representative optical micrographs of the samples are shown in Figs. 4 and 5. Fig. 6 shows representative scanning electron micrographs of the microstructure at different locations on the sample surface of sample 3. Polished surfaces of all of the consolidated samples reveal near-uniform grain size (Figs. 4 and 5). All the five molybdenum samples examined reveal a population of fine grains having near-uniform size with well-defined grain boundaries.

Fig. 6 shows representative microstructure, observed in the SEM, at different locations on polished and etched surface of sample 3. Identical microstructural features were observed for all five consolidated samples. The presence of clean grain boundaries in all the consolidated specimens confirms an activation of the powder particle surfaces that takes place to facilitate enhanced densification. The nature of interparticle regions in the green body compact is largely dependent on the conjoint and mutually interactive influences of size, shape and pressure experienced by the powder particles during consolidation. Prior to actual consolidation, the green compact comprises a random distribution of interparticle contacts with a population of voids between the powder particles. The interparticle contacts

serve as potential sites for high local stress concentration. In pressure-assisted consolidation, even nominal low stresses are adequate enough to enhance the densification of powders due to the presence of high local stress concentrations. When the interparticle contact is small, the effective stress at the contact is high and decreases as the contact grows in size. Flow of current through the compact causes the interparticle contact zone to be heated up faster than the interior of powder particle and the interparticle gap. The highly localized heating aids in softening the interparticle contact. Subsequent application of an external pressure and a DC voltage facilitates powder particle rearrangement and densification by inducing localized heating and promoting plastic deformation at all areas of interparticle contact. Since the present technique of P<sup>2</sup>C relies on rapid consolidation (a fraction of total cycle time) and the isothermal holding time is only a few minutes, the energy (thermal plus mechanical) available at the interparticle regions is sufficient to facilitate complete particle contact.

#### 3.2. Density

To establish the influence of pulsing on overall densification, samples 2 and 4 were consolidated without any pulse. Sample 1 was consolidated under conditions of pulse and an isothermal hold time of 1 min with a resultant density of 98.5%. Sample 2 was consolidated without pulse and an isothermal hold time of 1 min, and had a density (98%) close to that of sample 1. Sample 3, which was consolidated at a slightly lower pressure (40 MPa) and with the aid of pulse, revealed density different from sample 4 consolidated at the same pressure but under conditions of no-pulse. Sample 3 had a density of 96%, while sample 4 had a density of 93%. The net effect of application of a pulse on densification was pronounced at the lower pressure.

Initial packing of powder particles in the green compact has a network of contacting particles and interparticle

Table 2  
Nanohardness and elastic modulus of the consolidated molybdenum samples

Sample	Process conditions	Nanohardness (GPa)	Elastic modulus (GPa)
1	Pulse; 1650°C, 1 min, 48 MPa	3.44	344.0
2	No-Pulse; 1650°C, 1 min, 48 MPa	3.86	361.0
3	Pulse; 1600°C, 1.5 min, 40 MPa	3.43	337.0
4	No-Pulse; 1650°C, 1.5 min, 40 MPa	3.37	344.0
5	Pulse; 1650°C, 2 min, 40 MPa	3.64	336.0

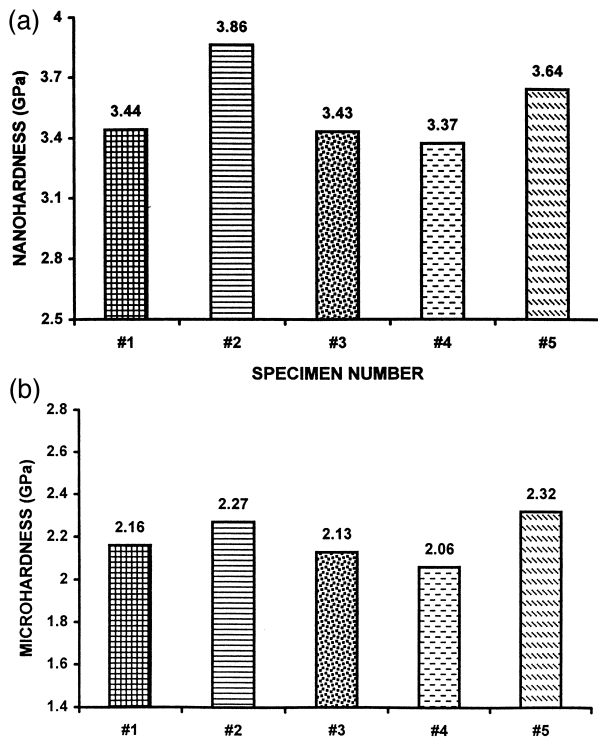


Fig. 8. (a) Bar graph comparing the nanohardness of the five samples of molybdenum. (b) Bar graph comparing the microhardness of the five samples of molybdenum.

voids. For simplicity, the network of particle contacts is shown in Fig. 1 for the case of spherical particles. However, in an actual scenario, there exist particles having varying sizes and shapes. Consequently, the pressure that is concentrated at the interparticle contacts depends upon both the size and shape of the powder particles.

It is well known that the yield strength of a metal decreases with an increase in temperature. Fine powders of a metal can be densified to nearly 100% density by inducing plastic flow at pressures far above the yield strength, which decreases at the higher temperature [24]. During the second stage of consolidation, an initial densification of the particles is favored by their rearrangement coupled with the occurrence of flow and deformation at the interparticle contacts. This effectively determines both the nature and quality of particle bonds. When a large current passes through the compact, there occurs heterogeneous surface heating of the powder particles. Particle surfaces and interparticle contacts are heated quickly while concurrently maintaining a relatively low temperature within the particle interior. Conjoint application of a uniaxial pressure causes more and more of the particles to come into contact and the material easily flows into pores and interparticle voids due to plastic deformation. Since densification occurs at a rapid rate, the particles have little time to increase their size, minimizing the possibility of grain growth.

### 3.3. Hardness

#### 3.3.1. Nanoindentation results

A typical load–displacement curve from a nanoindentation test on a molybdenum sample (sample 1) is shown in Fig. 7. The nanoindentation test results on the five molybdenum samples are summarized in Table 2. Even though the indentation sites on these samples were randomly chosen, there is minimum scatter in the hardness measurements. The overall hardness of sample 1 is 3.44 GPa, while that of sample 2 is 3.86 GPa. The hardness of sample 3 consolidated at the lower temperature (1600°C) and pressure (40 MPa) is quite close to that of sample 1 and inferior to sample 2 (3.86 GPa) (no-pulse,  $T = 1650^\circ\text{C}$  and pressure = 48 MPa). Hardness of the five samples is compared in the bar graph shown in Fig. 8a.

Elastic modulus, as measured by the nanoindentation technique, of the five samples is shown in the bar graph in Fig. 9. Elastic modulus of the pulsed molybdenum sample (sample 3) ( $E = 337$  GPa) is inferior to that of the no-pulse counterpart (sample 2,  $E = 361$  GPa). Also, the sample consolidated at  $1650^\circ\text{C}$  had a marginally higher elastic modulus than the sample obtained by consolidating at  $1600^\circ\text{C}$ . Overall, the elastic modulus values accord well with established values for polycrystalline molybdenum and molybdenum alloys. The state of stress in the immediate vicinity of the indenter is complex and compressive directly under the tip. It is expected that the microscopic cracks, emanating from the pores, would remain closed in pure compression and would not greatly affect the value of elastic modulus measured by nanoindentation.

**3.3.1.1. Microhardness.** Vickers microhardness measurements made at different locations on the surface of each sample are summarized in Table 3. Since the samples were metallographically polished to a perfect mirror finish, the variability in measured hardness values at different locations on the sample surface was less pronounced in the as-compacted molybdenum samples (Fig. 10) and the mea-

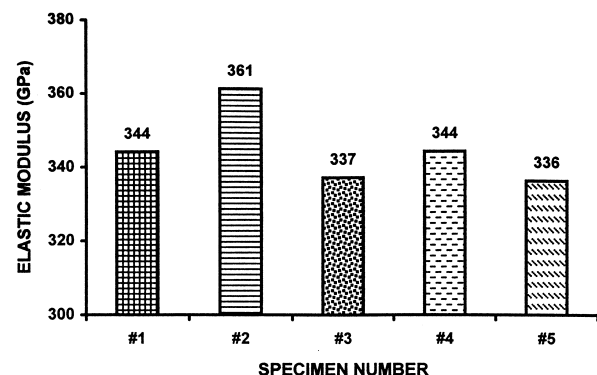


Fig. 9. Bar graph comparing the elastic modulus (GPa) of the five samples of molybdenum.

Table 3  
Vickers microhardness measurements on the consolidated molybdenum samples

Sample	Process conditions	Microhardness (GPa)					Average
		Trial 1	Trial 2	Trial 3	Trial 4	Trial 5	
1	Pulse; 1650°C, 1 min, 48 MPa, 4000 A, 5.5 V	219	216.7	221.3	219	225.9	220.42 (2.16 GPa)
2	No-Pulse; 1650°C, 1 min, 48 MPa, 4000 A, 5.7 V	225.1	237.4	231.5	231.5	231.5	231.40 (2.27 GPa)
3	Pulse; 1600°C, 1.5 min, 40 MPa, 4000 A, 5.6 V	212.4	211.7	212.4	227.5	222.0	217.20 (2.13 GPa)
4	No-Pulse; 1650°C, 1.5 min, 40 MPa, 4000 A, 5.5 V	193.6	213.8	216.0	210.9	216.0	210.00 (2.06 GPa)
5	Pulse; 1650°C, 2 min, 40 MPa, 4000 A, 5.5 V	256.30	249.7	217.5	249.70	208.10	236.26 (2.32 GPa)

sured microhardness was observed to be near-uniform throughout each as-compacted sample, indicating uniform densification. Polishing of the sample surface facilitates reducing the spread in measured hardness values. Sample 5, obtained by consolidating the molybdenum powders at 1650°C and a uniaxial pressure of 40 MPa, with an isothermal holding time of 2 min, exhibited a hardness of 2.32 GPa. Sample 2, consolidated under conditions of no-pulse using a pressure of 48 MPa, exhibited a marginally higher value of hardness (2.276 GPa) than sample 1 (2.16 GPa), which was consolidated under conditions of pulse at an identical pressure (48 MPa). The situation was found to be different for samples 3 and 4, both of which were consolidated at 40 MPa and an isothermal hold time of 1.5 min. The hardness of sample 3, consolidated in the pulse condition, was marginally higher (2.13 GPa) than that of sample 4 (2.06 GPa) obtained by consolidating in the no-pulse condition. The hardness values of the samples consolidated under pulse and no-pulse condition, at the different pressures, are shown in Fig. 8b. On account of the higher load used to indent the sample in the Vickers microhardness test when compared to the load used in the nanoindentation test, the corresponding area and depth of indent on the sample surface are larger than in the case of the nanoindentation test. Contributions from “local” microstructural heterogeneities and artifacts such as microscopic voids, pores and fine microscopic cracks are responsible for the observed lower value of the microhardness of the sample in comparison to the nanohardness.

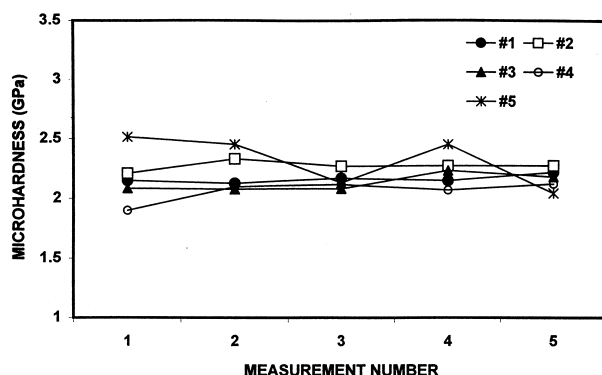


Fig. 10. Microhardness traverse across the molybdenum samples showing absence of spatial variability.

Microhardness measurements made on molybdenum have been reported to vary with the consolidation process technique used [25–27]. Tuominen and Dahl [25] reported microhardness values for unsintered molybdenum powder extrusions (about 270 HV 10), and conventionally processed powder metallurgy molybdenum bars (about 250 HV 10). Wangwiwat and Murr [26] reported hardness values of about 390–188 HV 50 for explosively shock-loaded rolled molybdenum sheet with as-fabricated or annealed grain sizes ranging from 1 to 67  $\mu\text{m}$ . Murr et al. [27] also reported hardness values ranging from 340 to 390 HV 50 for shock-loaded molybdenum having a 1  $\mu\text{m}$  grain size. The microstructure of explosively shock-loaded rolled molybdenum sheet [27] comprised dislocation tangles and a high density of dislocation loops. Murr et al. [27] reported a high density of dislocation loops to be incorporated well within the dislocation structure of subgrain boundaries of explosively consolidated molybdenum powders. Hence, the presence of a subgrain structure coupled with a high defect structure, in explosively consolidated molybdenum, was responsible for the reported higher range of microhardness values [27]. In this research study, the microhardness values measured at different locations of each sample were essentially uniform, unlike the findings made on explosively consolidated molybdenum powder and sheet.

#### 4. Conclusions

Based on the results obtained in an experimental study aimed at understanding the influence of process conditions on microstructure and hardness of molybdenum samples made by consolidating powders of molybdenum, the following are the key observations.

(1) Molybdenum powders were successfully consolidated by the technique of  $P^2C$ .

(2) Samples consolidated at the temperature of 1650°C and pressure of 48 MPa for a time period of 1–2 min had a theoretical density of 98%.

(3) Sample consolidated at 1650°C and a pressure of 40 MPa for a time period of 2 min had the maximum microhardness of 2.32 GPa.

(4) Microhardness values measured at different locations on the surface of the consolidated specimen were

consistent and revealed that uniform and porosity-free densification of the powder particles had occurred during consolidation.

(5) On account of the higher load used to indent the sample in the Vickers microhardness test when compared to the load used in the nanoindentation test, the corresponding area and depth of indent on the sample surface are larger than in the case of the nanoindentation test. Contributions from “local” microstructural heterogeneities and artifacts such as microscopic voids, pores and fine microscopic cracks are responsible for the observed lower value of the microhardness of the sample in comparison to the nanohardness.

## References

- [1] E.R. Braithwaite, J. Haber, Molybdenum: An Outline of its Chemistry and Uses, Elsevier, New York, 1994.
- [2] S. Nemat-Nasser, W. Guo, M. Liu, Experimentally based micromechanical modeling of dynamic response of molybdenum, *Scr. Mater.* 40 (1999) 859.
- [3] J.A. Shields Jr., E.L. Baker, Molybdenum alloys and emerging applications, *Adv. Mater. Process.* 1 (1999) 61.
- [4] S.R. Chen, P.J. Maudlin, G.T. (Rusty) Gray III, Mechanical properties and constitutive relations for molybdenum under high strain-rate deformation, in: A. Crowson, E.S. Chen, J.A. Shields, P.R. Subramanian (Eds.), *Molybdenum and Molybdenum Alloys*, TMS, Warrendale, PA, 1998, p. 155.
- [5] E.L. Baker, A. Daniels, G.P. Voorhis, T. Verong, in: A. Crowson, E.S. Chen, J.A. Shields, P.R. Subramanian (Eds.), *Molybdenum and Molybdenum Alloys*, TMS, Warrendale, PA, 1998, p. 200.
- [6] E.L. Kemer, D.L. Johnson, *Am. Ceram. Soc. Bull.* 64 (1985) 1132.
- [7] R.F. Cheney, *Sintering of Refractory Metals*, 9th edn., Metals Hand Book 7 ASM, Metals Park, OH, 1984, p. 389.
- [8] L.E. Murr, in: M.A. Meyers, L.E. Murr (Eds.), *Shock Waves and High Strain-Rate Phenomena: Concepts and Applications*, Plenum, New York, NY, 1981.
- [9] M.A. Meyers, B.B. Gupta, L.E. Murr, *J. Met.* 33 (10) (1981) 21.
- [10] D. Raybould, D.G. Morris, G.A. Cooper, *J. Mater. Sci.* 14 (1979) 2523.
- [11] A.M. Staver, in: M.A. Meyers, L.E. Murr (Eds.), *Proc. Int. Cogence Shock Waves High Strain-Rate Phenom. Met.*, Plenum, New York, 1981, p. 865.
- [12] P. KasiRaj, P. KasiRaj Jr., R.B. Schwarz, T.J. Ahrens, *Journal of Materials Science* 32 (1984) 1235.
- [13] R.V. Raman, *Adv. Mater. Process.* 137 (1990) 109.
- [14] C.A. Kelto, E.E. Timm, *Annu. Rev. Mater. Sci.* 19 (1989) 527.
- [15] G. Jones, J.R. Groza, K. Yamazaki, K. Shoda, Plasma-activated sintering of tungsten powders, *Mater. Manuf. Process.* 9 (1994) 1105.
- [16] J.R. Groza, S. Risbud, K. Yamazaki, *J. Mater. Res.* 7 (1992) 2643.
- [17] B.G. Ravi, P.D. Ramesh, N. Gupta, K.J. Rao, Microwave-assisted preparation and sintering of Al<sub>2</sub>O<sub>3</sub>, ZrO<sub>2</sub> and their composites from metalorganics, *J. Mater. Chem.* 7 (1997) 2043.
- [18] B.G. Ravi, V. Praveen, M. Pannerselvam, K.J. Rao, Microwave-assisted preparation and sintering of mullite composites from metalorganics, *Mater. Res. Bull.* 33 (1998) 1527.
- [19] R. Kalyanaraman, S. Yoo, M.S. Krupasankara, T.S. Sudarshan, R.J. Dowding, *Nanostruct. Mater.* 10 (1998) 1379.
- [20] S.H. Yoo, T.S. Sudarshan, K. Sethuram, G. Subhash, R.J. Dowding, Dynamic compression behavior of tungsten powders consolidated by plasma pressure compaction, *Powder Metall.* 42 (2) (1999) 181–182.
- [21] M.F. Doerner, W.D. Nix, *J. Mater. Res.* 1 (1986) 601.
- [22] W.C. Oliver, G.M. Pharr, *J. Mater. Res.* 7 (1992) 1564.
- [23] M.M. Krushchov, E.S. Berkovich, *Ind. Diamond Rev.* 11 (1951) 42–49.
- [24] R.M. German, *Rev. Part. Mater.* 2 (1994) 117.
- [25] S.M. Tuominen, J.M. Dahl, 108th AIME Annual Meeting, New Orleans, LA, February, 1979.
- [26] K. Wangwiwat, L.E. Murr, Shock-induced cracks in molybdenum sheet, *J. Appl. Phys.* 50 (2) (1979) 813–816.
- [27] L.E. Murr, S.M. Tuominen, A.W. Hare, S.H. Wang, Structure and hardness of explosively consolidated molybdenum, *Mater. Sci. Eng.* 57 (1983) 107.